

**MEASUREMENTS OF LITHOSPHERIC FLEXURE DUE TO LATE AMAZONIAN SUBSIDENCE OF OLYMPUS MONS.** D. J. Chadwick<sup>1</sup>, P. J. McGovern<sup>2</sup>, M. C. Simpson<sup>1</sup>, and A. Reeves<sup>1</sup>, <sup>1</sup>Department of Geology, College of Charleston, 66 George St., Charleston, SC 29424; chadwickj@cofc.edu, <sup>2</sup>Lunar and Planetary Institute, Universities Space Research Association, 3600 Bay Area Blvd., Houston, TX, 77058.

**Introduction:** Olympus Mons is the largest volcano in the solar system, with a basal diameter over 600 km and a height over 23 km above the surrounding plains. The volcano has a long history of activity dating to the Noachian, and crater counts for the calderas and lower flank flows reveal more recent volcanic activity clustered around 100-200 Myr and as young as 2.5 Myr [1, 2]. Faulting of the edifice also suggests recent flank spreading and intrusion [3]. These relatively young features suggest that a significant magmatic volume has been added to the volcano in the past 200 Myr.

In this study, paleotopographic methods and flexural modeling were used to identify and constrain the magnitude of subsidence of Olympus Mons that may be the result of this recent activity. Thermal Emission Imaging System (THEMIS) and Mars Orbiter Laser Altimeter (MOLA) data were used to map the orientations of dozens of long (42.6 - 220.4 km), thin lava flows on the plains just to the south and southeast of the flanks of Olympus Mons (Figure 1). These flows originated from small vents to the east of Olympus Mons and flow from northeast to southwest around its flank, occupying about 1/3 of the flexural trough that surrounds the edifice. They represent the local slope direction at the time they were emplaced. These orientations were compared with modern topographic slopes measured in MOLA data at the same locations, to identify changes in the topography that might have resulted from subsidence of Olympus Mons. Flexural modeling was then employed to calculate the magnitude of intrusion required to account for the subsidence.

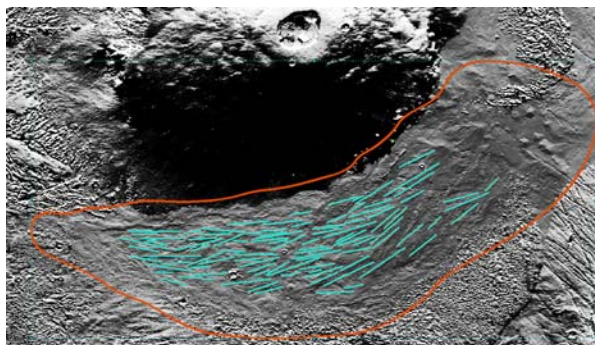


Figure 1. Vectors showing locations of 94 lava flows used in this study. These flows are no longer aligned with modern topography. Olympus Mons at top.

**Methods:** The azimuths of the lava flows (indicating paleoslopes), in conjunction with the MOLA topography [4] (indicating the current slopes) were used to invert for the dimensions of the volcanic material added to Olympus Mons that would account for the observed slope changes. This is a five-step process:

Step 1: The azimuths of lava flows were collected on the plains adjacent to the southern and southeastern flanks of the volcano to identify the original downhill directions of the flows (Figure 1). The head and terminus points of 94 long (>40 km), narrow flows with relatively uniform azimuth directions were digitized in ArcMap (Mars 2000 datum).

Step 2: MOLA points within 30 km of each mapped flow azimuth datum (location at head of the flow) were extracted to create a reference surface. The slope magnitude and azimuth of that plane were then calculated to derive the modern topographic values.

Step 3: Vertical displacements resulting from a lithospheric flexure model were calculated, a long-wavelength response of the relatively thick Martian lithosphere to the addition of basaltic magmas on Olympus Mons and the flexural trough surrounding the edifice. A “shallow spherical shell” loading model [5] was used, with load dimensions (radius  $r_m$  and height  $h_m$ ), and elastic lithosphere thickness ( $T_e$ ) used as model inputs.

Step 4: To remove the effects of the loading-induced flexure, the vertical displacements of each individual model were subtracted from the MOLA topography, yielding a “pre-deformation” surface. To calculate the pre-deformation downslope azimuths (and slope magnitudes), the same calculation was performed as in Step 2, but using the modeled pre-deformation topography. The misfit between the pre-deformation surface downhill azimuths and the flow unit azimuths is then calculated (Figure 2).

Step 5: Probability density functions for model radius and height parameters ( $r_m$  and  $h_m$ ) were calculated using a “bootstrap” method [6], for which random resampling of the flow points is used to create multiple synthetic datasets. For each synthetic dataset, random combinations of model parameters are calculated, and the combination with the lowest r.m.s. misfit is kept. The distributions of parameters for the kept parameters over all the synthetic datasets (Figure 3) were converted into probability density functions.

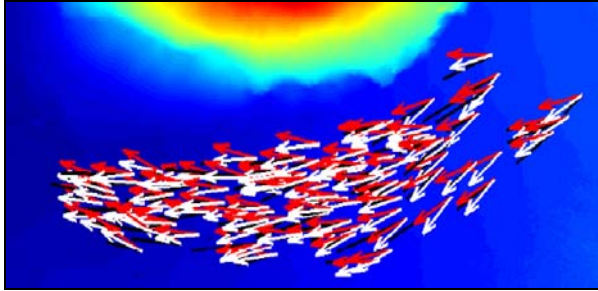


Figure 2. Basemap of MOLA topography. Paleoslope orientations are denoted by black lines connecting the beginning and endpoints of mapped flows. The figure shows paleoslopes (black lines), the current downhill direction from MOLA (red arrows), and pre-deformation downhill direction determined from a flexural loading model (white arrows).

**Results:** The results of the initial mapping show that all 94 of the flows are no longer oriented in a downhill direction, that modern slope directions are rotated in a clockwise direction relative to the paleoslopes, and these orientations are consistent with subsidence centered on Olympus Mons in the time since the flows were emplaced. Our preliminary geophysical modeling used a range of load volumes, load radii, and lithospheric thicknesses to identify the scenario required to best restore modern topography to match the paleo-topography present when the lava flows were emplaced. The nominal best-fit height for the limited inversion is 2.85 km, a significant fraction of Olympus Mons' current topographic height. This finding implies a significant volcanic flux late in the history of the edifice.

Our new crater size-density measurements (Figure 3) of the plains in the study area show that the observed subsidence occurred within the past  $229 \pm 26$  my (late Amazonian), although the subsidence could have occurred any time over that period. Previous crater counts for Olympus Mons calderas and lower flank flows [1,2] reveal volcanic activity clustered around this same time period and younger (100-200 Myr). The correspondence between this period of extensive extrusive activity on Olympus Mons and the subsidence of the surrounding plains identified in this study strongly suggests a link between these two events.

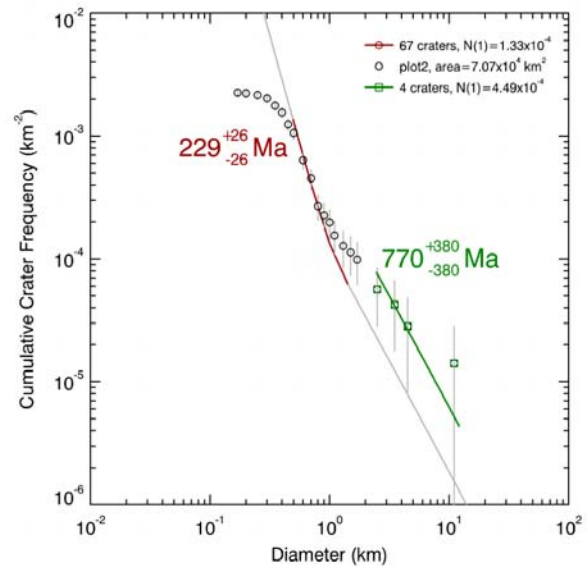


Figure 3. Craters in the study area were mapped using CraterTools and CraterStats software to establish the age of the subsided terrain and to constrain the timing of the subsidence. Crater size-density plot shows the observed subsidence occurred within the past  $229 \pm 26$  Myr, consistent with other indications of volcanic and tectonic activity on Olympus Mons.

**References:** [1] Neukum et al., (2004) *Nature*, 432, 971-979. [2] Robbins et al., (2011) *Icarus*, 211, 1179-1203. [3] Basilevsky et al., (2006) *GRL*, 33. [4] Smith et al., 2001. [5] Brothie and Sylvester, 1969. [6] Menke, 2012.